Soft Matter

Accepted Manuscript

ROYAL SOCIETY OF CHEMISTRY

www.rsc.org/softmatter

Femtosecond Laser Controlling Wettability of Solid Surfaces

Jiale Yong, Feng Chen*, Qing Yang*, and Xun Hou

Key Laboratory of Photonics Technology for Information of Shaanxi Province & State Key Laboratory for Manufacturing System Engineering, School of Electronics & Information Engineering, Xi'an Jiaotong University, Xi'an, 710049, P. R. China

*Corresponding author: chenfeng@mail.xjtu.edu.cn (F. Chen)
yangqing@mail.xjtu.edu.cn (Q. Yang)

Abstract

Femtosecond laser microfabrication is emerging as a hot tool for controlling the wettability of solid surfaces. This paper introduces four typical aspects of femtosecond laser induced special wettability: superhydrophobicity, underwater superoleophobicity, anisotropic wettability, and smart wettability. The static property is characterized by contact angle measurement, while the dynamic feature is investigated by the sliding behavior of a liquid droplet. Using different materials and machining methods results in different rough microstructures, patterns, and even chemistry on the solid substrates. So, various beautiful wettabilities can be realized because wettability is mainly dependent on the surface topography and chemical composition. The distinctions of the underlying formation mechanism of those wettabilities are also described in detail.

1. Introduction

Wettability plays a very important role in creature's survival and our daily life.[1-10] Recently, much attention has been paid to fabricate special wettable surfaces due to their significance in basic researches, practical applications, and bionics.[11-20] Four typical aspects of wettability are widely studied by researchers, including superhydrophobicity, superoleophobicity, anisotropic wettability, and smart wettability. A surface with water contact angle (WCA) larger than 150° is generally defined as a superhydrophobic surface.[21-24] Superhydrophobicity is the earliest one studied. If the liquid object is another most popular liquid in daily life: oil, the oil-repellent surface is called superoleophobic surface. Following the same principle of superhydrophobicity, superoleophobicity is the same as an oil droplet showing oil contact angle (OCA) higher than 150°.[25-28] In nature, a water droplet on the rice leaf has different WCA values, as well as sliding angles (SAs), along two vertical directions, respectively.[29-31] The anisotropic property is caused by the ordered arrangement of the rough micro-papillas on rice leaves. The static characteristic (anisotropic wetting) and the dynamic feature (anisotropic sliding) are two forms of anisotropic wettability. In addition, some intelligent surfaces show

"smart wettability"; that is, the wettability of those surfaces can be reversible switched through responding to external stimulus, such as light,[32,33] pH,[34,35] thermal,[36,37] electricity,[38,39] force,[40,41] etc. Smart wettability has been artificially achieved but not observed in nature.[14] Up to now, many techniques have been developed to obtain the above-mentioned wettabilities, such as template imprinting,[42,43] self-assembly method,[44,45] chemical etching,[46,47] photolithography,[48,49] plasma etching,[50,51] and electrospinning.[52,53]

In the past decade, femtosecond laser microfabrication has been applied in interface science to control the solid surfaces' wettability.[54-63] This technology can directly create micro/nanoscale hierarchical structures on a wide variety of materials by a simple one-step scanning method.[54,57,58,61,63] By combining the femtosecond laser system with the computer controlled three-dimensional translation stage, the laser processing position, scanning speed and scanning track can be precisely controlled by computer program. Various pre-designed patterns were prepared by this technology without the need for a harsh machining environment and expensive masks (Figure 1). Since the wettability is governed by not only the chemical composition but also the surface topography, those pattern structures usually exhibit various special wetting properties.[65-68]

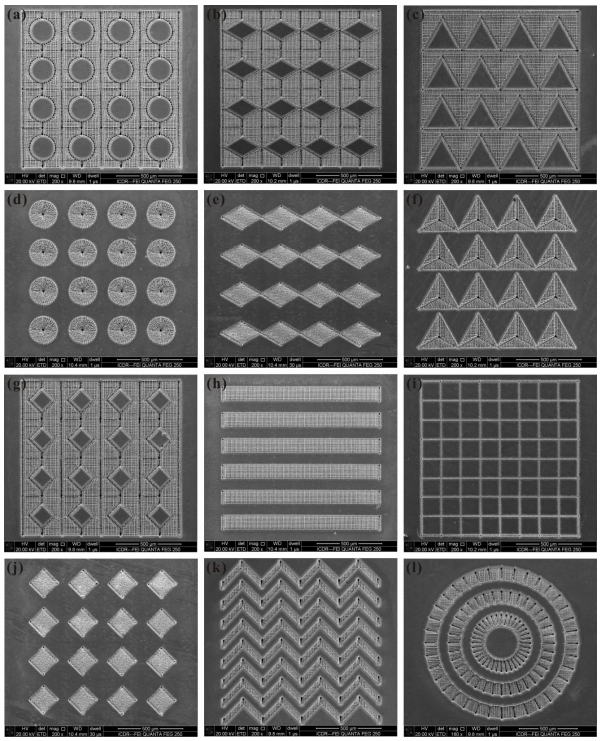

Figure 1. Various patterns prepared through femtosecond laser microfabrication on Ti sheet. (Reproduced from ref. 58 with the permission of RSC.)

This paper provides an introduction of employing femtosecond laser to realize special wettabilities. According to the characteristic of different wettabilities, we divide this article into four parts, which respectively focus on superhydrophobicity, underwater superoleophobicity, anisotropic wettability, and smart wettability. The formation mechanism of those properties is from simple to complex, while the

function of those surfaces develops from single to multiple. With the price of femtosecond laser system decreasing year by year, more and more laboratories have their own femtosecond laser equipment. This article should provide a useful guide for the integrated field of femtosecond laser microfabrication and wettability, and attract more researchers to work on this interesting research area.

2. Controlling wettability by femtosecond laser

2.1 Superhydrophobicity

The most famous superhydrophobic surface is lotus leaf which surface is covered with micro/nanoscale hierarchical papillas and a hydrophobic wax crystal layer.[29,69] The combination of rough microstructures and hydrophobic chemistry endows lotus leaf with water repellent ability because the real contact area between water droplet and lotus leaf is greatly reduced. Inspired by nature, there are main two routes to design artificial superhydrophobic surfaces: modifying rough surface by materials with low surface energy; constructing rough microstructures on hydrophobic substrate.[65-68]

Mazur et al. and Stratakis et al., respectively, prepared superhydrophobic Si surfaces by femtosecond laser irradiation under reactive SF_6 gas.[70,71] The laser induced structure is composed of microscale conical spikes, arranging as a spikes forest, as shown in Figure 2a,b. The average size of the spikes is 10 μm and the aspect ratio is about 4. There are abundant nanoprotrusions with the size of a few hundred nanometers covering on every spike. After fluoroalkylsilane modification, the two length-scale rough surface shows a WCA of 154° ± 1° and a very small SA of 5° ± 2°. Both the artificial microstructure and the water-repellent characteristic are very similar to a natural lotus leaf.[71] However, the SF_6 gas results in complex experiment equipment and fabrication process. It is of great significance to develop a simple way to prepare superhydrophobic surfaces in ambient environment using a femtosecond laser.

We recently reported a self-organized rough micro-mountain array structure which was fabricated by femtosecond laser irradiating Si surface in atmosphere environment, as shown in Figure 2c-f.[72,73] The diameter and height of the rough micro-mountains are 6 μm and 2.9 μm, respectively. The micro-mountains arrange neatly and form a square array with period of 10 μm. The surface roughness is about 2.46 μm. The inset in Figure 2d shows the image of a 9 μL water droplet lying on the fluoroalkylsilane modified rough surface, with WCA of 158° ± 1°. Water droplets on the surface can roll off easily as soon as the sample is tilted 4°. The surface shows superhydrophobicity and ultralow water adhesion, agreeing well with the Cassie contact state.[74,75] The water droplet only contacts the peak of the rough microstructures. An air cushion is trapped between the droplet and the rough surface. This air cushion endows the femtosecond laser induced surface with excellent water-repellent property.

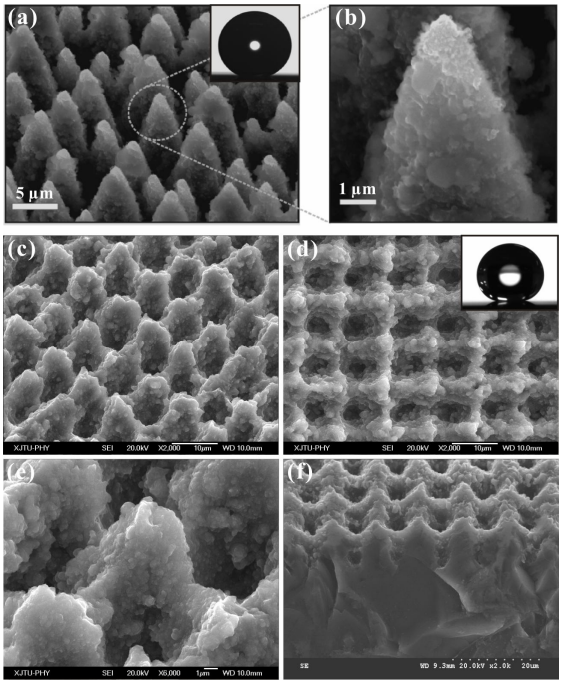

Figure 2. Typical SEM images of the Si surfaces irradiated by femtosecond laser under SF_6 gas (a,b) and in air environment (c-f), respectively. The insets show a water droplet on the corresponding surfaces. (Reproduced from ref. 71 and 72 with the permission of Wiley and Springer.)

The as-prepared superhydrophobic surfaces possess excellent self-cleaning ability.[72] If the surface is polluted by calcium carbonate powder and slightly tilted, water droplet located on the surface will roll off easily and take away the pollutants, leaving a clean path behind. Interestingly, the as-prepared surfaces still have superhydrophobicity for strong acid and alkaline solutions. This feature endows the surface with self-cleaning function even in acid or alkaline rain. In addition, this pH stability makes the superhydrophobic surfaces possible for applying to biological and chemical fields.

Superhydrophobicity can be directly achieved on hydrophobic materials without low surface energy modification compared with intrinsic hydrophilic substrates.[62] Figure 3a shows the SEM image of the femtosecond laser irradiated polydimethylsiloxane (PDMS) surface. There are many flower-like particles with size of several micrometers coving on the surface. The particles are decorating with abundant nanoscale protrusions. Water droplet on the surface shows a static WCA of 162° ± 1°, and can roll off with the sample being tilted 1°. The superhydrophobicity with ultralow adhesion indicates that the droplet on the sample is at Cassie state.[74,75]

We further weaved patterned PDMS surfaces consisting of periodic square array based on selective femtosecond laser irradiation technology (Figure 3b).[62] The femtosecond laser scanned domain is a micro/nanoscale hierarchical rough structure and shows ultralow adhesive superhydrophobicity. The rest non-irradiated flat PDMS performs intrinsic hydrophobicity (WCA = 110°). Figure 3c shows the variation of WCA/SA with the length (L) of the side of unstructured square when the period (T) of the square array is set at 200 μm. For a 7 μL water droplet, superhydrophobicity is

obtained with $L \leq 180$ μm. As far as the patterned surface with greater L, there is not enough laser irradiated rough area to realize superhydrophobicity; that is, the average roughness of the overall pattern surface is too low. The dynamic property of a water droplet on the structured surface was also investigated via its sliding behavior. Water droplet moves easily on the surface with $L \leq 140$ μm as soon as the surfaces are only slightly tilted or shaken (Figure 3d). As the L rises from 140 μm to 180 μm, SA increases from 10° ± 1.5° to 54° ± 3° and then to 90° (Figure 3e-g). SA = 90° means that the water droplet firmly pins on the sample even though the substrate is erected or turned upside down. The SA result reveals that the water adhesion of the superhydrophobic surfaces can be tuned from ultralow to ultrahigh. This adhesion controllability is realized by adjusting the area proportion of laser structured and non-structured regions, which show ultralow adhesion and ultrahigh adhesion, respectively. A water droplet on the heterogeneous patterned surfaces contacts both the flat and laser-induced rough domains. Those two contact state are respectively at Young and Cassie wetting model.[62] As the L increases, the area fraction of the laser structured domain (Cassie contact) will decrease. The decrease of the average surface roughness causes a decline of WCA. Whereas, the area fraction of the flat domain (Young contact) will increase, resulting in the increase of water adhesion or SA value. Using those as-prepared surfaces, droplet fast stop, small water droplet transfer, and controllable droplet bounce are achieved.[62] In addition, many other microstructures and patterns are also prepared and showed controllable adhesive superhydrophobicity.[61,63,76]

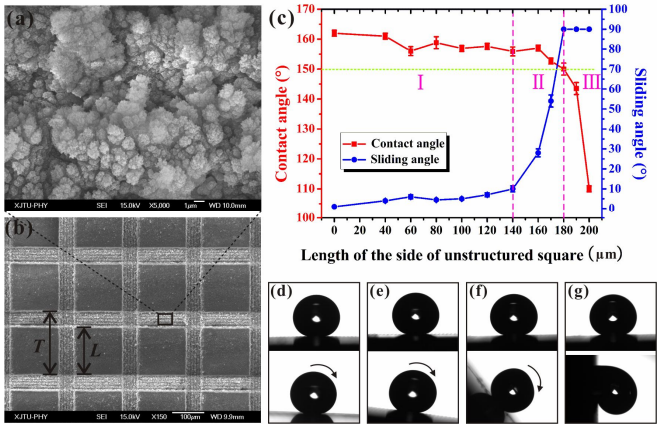

Figure 3. (a) SEM image of the PDMS microstructure ablated by femtosecond laser. (b) SEM image of the structured square array pattern. (c) WCA and SA values as a function of the L. (d-g) Shape and movement of a droplet on the square array surfaces: (d) L = 0 μm, (e) L = 140 μm, (f) L = 170 μm, and (g) L = 180 μm. (Reproduced from ref. 62 with the permission of ACS.)

2.2 Underwater superoleophobicity

Fish can swim freely in oil-spill water and avoid being polluted by oil because of the underwater superoleophobicity of its skin.[77] The unique ability is found from the synergy between the hierarchical rough microstructures and the hydrophilic chemistry of fish scales. The characteristic of fish scales suggests that surfaces that are

superhydrophilic in air are generally superoleophobic in water.

The femtosecond laser ablated micro-mountain array structures on Si surface (without fluoroalkylsilane modification) can also be used to obtain underwater superoleophobicity.[56] The flat Si surface shows weak hydrophilicity in air with a WCA of 60° (Figure 4a). If the flat sample is immersed in water, an oil droplet (1,2-dichloroethane) on the surface will keep more than half a nearly sphere (Figure 4c). The OCA is 124.6° ± 1°, showing ordinary oleophobicity in water. After femtosecond laser ablation, the wettability of the sample is enhanced by the hierarchical rough microstructures. Water droplet can spread out quickly on the laser ablated surface, exhibiting superhydrophilicity with WCA of 4° in air (Figure 4b). Interestingly, the laser induced surface shows superoleophobicity in water. Oil droplet can remain a spherical shape on the sample surface in water medium (Figure 4d). The OCA reaches up to 159.4° ± 1°. The surface also performs ultralow oil adhesion in water since the oil droplet can roll easily on a 0.5° tilted structured surface (Figure 4e). According to the underwater version of Cassie model, the rough microstructure is fully wetted by water.[56,77] The underwater oil droplet is supported by the micro-mountains and only touches the tip of the rough microstructures. A water cushion is trapped below the oil droplet. The trapped water endows the surface with underwater superoleophobicity because water naturally repels oil. Ultralow oil adhesion is a result of small contact area between underwater oil droplet and rough substrate. The hydrophilic silicon in air becomes oleophobic in water, while the oleophobicity is greatly amplified into underwater superoleophobicity by femtosecond laser induced rough microstructures.

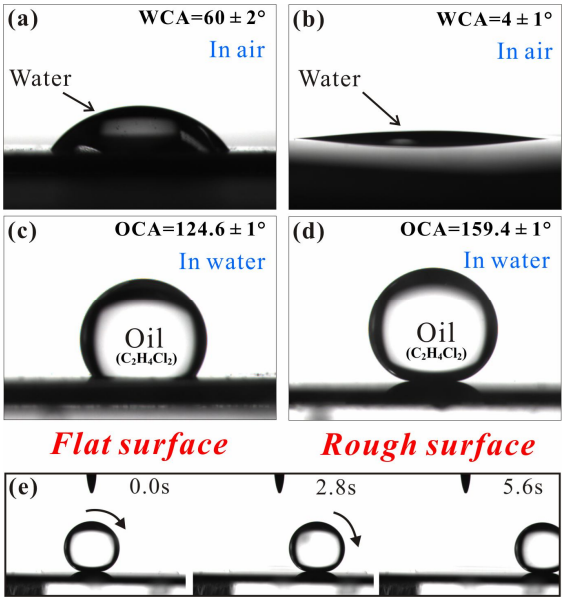

Figure 4. (a-d) Water wettability in air and underwater oil wettability of flat Si surface and laser induced rough Si surface, respectively. (e) Underwater oil droplet rolling on laser ablated sample tilted 0.5°. (Reproduced from ref. 56 with the permission of RSC.)

The transparent underwater superoleophobicity was also realized on silica glass surface.[57] Achieving underwater superoleophobicity and light transmission are

respectively taken inspiration from fish scales and *Diphylleia grayi*. The *Diphylleia grayi*'s petals are white in air, but on contact with water (such as in the rain) they become transparent, as shown in Figure 5a,b.[57] Because of the loose cell structure, water can enter the intercellular space of *Diphylleia grayi* petal on rainy days. A water-water interface displaces the initial water-air interface (in air), increasing light transmission so the petals turn transparent. Figure 5c shows the microstructure of the femtosecond laser ablated silica glass surface. Abundant irregular nano-particles disorderly distribute on the surface. When the laser ablated silica glass is immersed in water, the oil droplet on it keeps a spherical shape (Figure 5d). The OCA reaches up to 160.2° ± 1°, while the SA is only 1°, revealing an underwater superoleophobicity with ultralow oil-adhesion.

The transmittance of the rough silica glass is improved with shifting from atmosphere to water medium. When we put a paper with black letters behind the laser induced glass, the letters look obscure in air. After putting the sample in water, the letters "XJTU" becomes very clear (Figure 5e). The underwater oil droplet on the sample remains a small sphere (inset of Figure 5e). The remarkable transparency is confirmed by UV-vis spectra (Figure 5f). The underwater structured surface has a similar transmittance with bare flat silica glass in visible region. Water environment plays an important role in obtaining this good transparency. Like the *Diphylleia grayi* petals becoming transparent in the rain, the rough nanoscale structure of silica glass is wetted by water with immersing in water, forming a glass-water interface instead of glass-air interface. Since the refractive index of water is closer to silica glass than that of air, the degree of Mie scattering is effectively weakened, resulting in excellent transparency.[78,79]

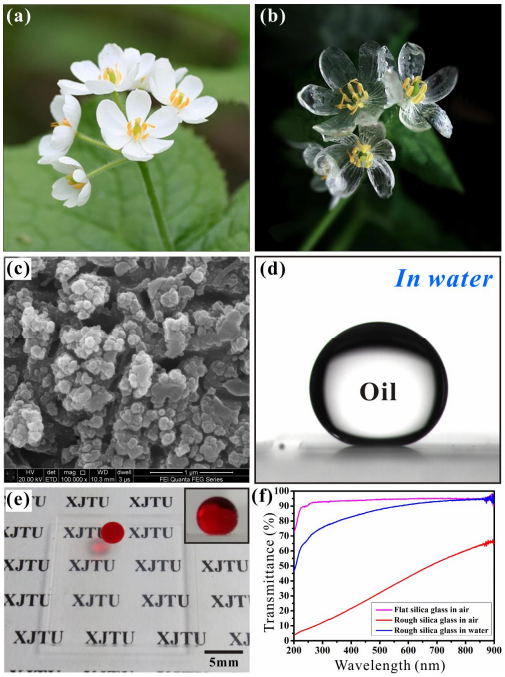

Figure 5. (a,b) Petals of *Diphylleia grayi*: (a) on a sunny day; (b) in the rain. (c) SEM image of the femtosecond laser irradiated silica glass surface. (d) Underwater oil droplet on the femtosecond laser irradiated silica glass. (e) High transparency of the laser induced surface in water medium. (f) UV-vis spectra of various silica glasses.

(Reproduced from ref. 57 with the permission of RSC.)

Controllable underwater oil-adhesion was realized on femtosecond laser ablated ordinary glass surfaces.[80] The resultant surfaces show micro/nanoscale binary rough topography and underwater superoleophobicity. By increasing the average distance of laser pulse focus, the underwater oil-adhesion increases from ultralow to ultrahigh because the oil droplet on the structured surfaces changes from underwater Cassie state to metastable state, and to underwater Wenzel state. The superoleophobic surface with low oil-adhesion is an ideal anti-oil-contamination layer in water. The superoleophobic surface with ultrahigh oil-adhesion can be applied in oil droplet transfer and even in the fusion of oil/organic microdroplets.

2.3 Anisotropic wettability

Slow femtosecond laser scan leaves a microgroove on the substrate surface. Using the line-by-line scanning mode, we obtained a periodic microgroove array on PDMS substrate, as shown in Figure 6a.[55] Every microgroove has a width of 12.17 μm and depth of 8.57 μm. In addition, many irregular nanoscale particles randomly decorate on the inside wall and out rim of the microgrooves.

Water droplet on the microgroove array structure is stretched along the microgrooves (Figure 6b). The anisotropic wettability of the groove-like microstructure is usually studied by measuring the perpendicular and parallel WCA/SA values.[30,73,81-83] The WCAs (SAs) perpendicular to and parallel to the microgrooves, respectively, defined as $WCA_{\perp}$ and $WCA_{//}$ ($SA_{\perp}$ and $SA_{//}$). Figure 6c shows the parallel view of a water droplet on the microgroove array surface with period (D) of 150 μm. The $WCA_{//}$ is 116.5° ± 2.5°. Whereas, the droplet along the perpendicular direction has a higher contact angle and $WCA_{\perp}$ is 134.8° ± 2.5° (Figure 6d). The degree of wetting anisotropy, $WCA_{\perp} - WCA_{//}$, is about 18.3°. Three main factors cause this anisotropic wetting phenomenon. Firstly, an energy barrier usually forms at the boundary between the laser-induced microgroove and the non-irradiated flat PDMS domain.[73,83,84] This energy barrier can prevent the water droplet spreading along the perpendicular direction, while there is no energy barrier along the parallel direction. Secondly, water droplet can partly dive into the rough microgrooves and is further driven to flow along the microgrooves by capillary action.[85-90] Finally, the three-phase contact line (TCL) is continuous along the microgrooves.[91] It is better for the droplet spreading and moving forward.

Figure 6e,f describe the rolling process of a water droplet on the microgroove array surface (D = 25 μm) along the parallel and perpendicular directions, respectively. The $SA_{//}$ is 31° ± 3°, while the $SA_{\perp}$ is about 76° ± 5°. The result shows that droplet prefers to move along the grooves direction. The SA difference reaches up to 45°, but the value of rice leaf is only 6°. A continuous short TCL always endows the surfaces with excellent water-shedding property.[91] Water droplet on the microgrooves structure has a continuous TCL along the parallel direction. However, the TCL along the perpendicular direction is very discontinuous and looks longer. Stronger hysteresis

effect forms in the perpendicular direction, resulting in water droplet rolling along this direction being more difficult than along the parallel direction.

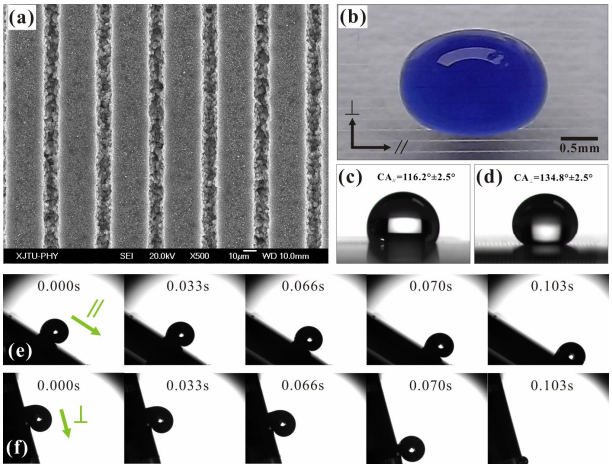

Figure 6. (a) SEM image of femtosecond laser induced microgroove array with D = 40 μm. (b) Blue-dyed water droplet on the microgroove array surface. (c,d) Water droplet on the microgrooves patterned surface (D = 150 μm) viewed from the parallel (c) and perpendicular (d) directions. (e,f) Droplet rolling on the microgroove array (D = 25 μm) along the parallel and perpendicular directions. The sample is respectively titled 31° (e) and 76° (f). (Reproduced from ref. 55 with the permission of RSC.)

The femtosecond laser induced microgroove array structure can also be immersed in water to control oil wettability.[92] We fabricated similar microgroove array on Si substrate and realized underwater anisotropic oil-wetting. For the sample with D = 450 μm, the OCAs parallel to and perpendicular to the grooves are 135.7° ± 1.5° and 155.5° ± 1.6°, respectively. The contact angle along the parallel direction is significantly smaller than that along the perpendicular direction, revealing the oil droplet tends to spread along the microgrooves. The degree of wetting anisotropy can be controlled from 0° to 19.8° by the period of the microgroove arrays.

Butterfly avoids being "shot down" by raindrops due to the directional adhesion of its wings.[93] Inspired by butterfly wings, a kind of triangle array patterns was constructed on PDMS material based on selective femtosecond laser irradiation.[94] The untreated triangle array is flat hydrophobic PDMS, while the surrounding domain is induced by femtosecond laser and shows superhydrophobicity. The droplet on the sample rolls along one direction distinctly easier than its opposite direction when the droplet and single hydrophobic triangle have comparable size. This special anisotropic wettable phenomenon is usually called "directional adhesion".[93] The obtained sliding anisotropy can even reach up to 21°. The directional adhesion results from the direction-dependent arrangement of hydrophobic triangles because the water droplets rolling along those two opposite directions have different TCL situations.

2.4 Smart wettability

Switchable wettability was realized on femtosecond laser ablated Ti surfaces.[58] As shown in Figure 7a,b, the laser induced morphology is the typical rough

micro-mountain arrays. The laser ablated sample consists of both Ti and a new element O instead of pure Ti. Their atomic proportions are 51.81% and 48.19%, respectively. Oxidation and hierarchical rough microstructure formation synchronously happen during the femtosecond laser ablation, constructing a rough TiO_2 layer covering on the original substrate.

The laser-induced surface initially shows superhydrophobicity with WCA of 154.5° ± 2.5° (Figure 7c). A mirror-like interface can be seen with immersing the sample in water, revealing the laser-irradiated Ti is a Cassie surface.[95] After UV irradiation for 40 min, the WCA decreases to 2.5° (Figure 7d). At present, the sample submerging in water does not show silver mirror. The wettability is switched from superhydrophobicity to superhydrophilicity in air. Furthermore, the sample can re-obtain superhydrophobicity through dark storage for 2 days.

The switching trend of oil wettability in water is opposite to that of water wettability in air. The laser-induced sample incipiently presents underwater superoleophilicity (Figure 7e). The underwater oil droplet will spread out quickly with OCA of near 4° once it contacts the submerged rough TiO_2 surface. After UV light irradiation, the wettability of the sample switches to underwater superoleophobicity (Figure 7f). The underwater oil droplet on the sample has an OCA of 160.5° ± 2° and can easily roll away if the sample is titled 1°. The underwater superoleophilicity can also be recovered by keeping the sample in dark for 2 days. Both the water wettability and the underwater oil wettability can be cycled many times. Similar property is also seen on femtosecond laser treated Zn surface.[59]

As shown in Figure 7g, femtosecond laser irradiation not only generates hierarchical rough microstructures but also oxidizes the Ti material. The laser induced rough TiO_2 layer shows ultralow water adhesive superhydrophobicity. According to the Cassie model, the water droplet only contacts the peak of the rough microstructures (Figure 7i).[74-76] An air cushion forms between water droplet and rough sample surface with submerging the as-prepared sample in water. When an underwater oil droplet contacts the surface, the oil will spread along and displace the trapped air for the pressure and capillary action, resulting in underwater superoleophilicity (Figure 7k). During UV light irradiation, the lattice oxygen combines with photogenerated holes to form oxygen vacancies on the TiO_2 surface.[96-101] The oxygen vacancies further turn into hydroxyl groups by dissociative adsorption of atmospheric water (Figure 7h). The hydroxyl groups make the rough TiO_2 surface present superhydrophilicity (Figure 7j). With immersing the sample in water, the microstructures are completely wetted and occupied by water. If an oil droplet is placed on the sample surface, a water cushion will be trapped between the oil droplet and the substrate (Figure 7l). The water cushion endows the sample with underwater superoleophobicity based on the underwater version of Cassie contact model.[56,77] For the dark storage process, the implanted hydroxyl moieties tend to be replaced by ambient oxygen.[96,97] As the hydrophobicity grows stronger, the sample recovers to its original superhydrophobic and underwater superoleophilic state (Figure 7i,k).

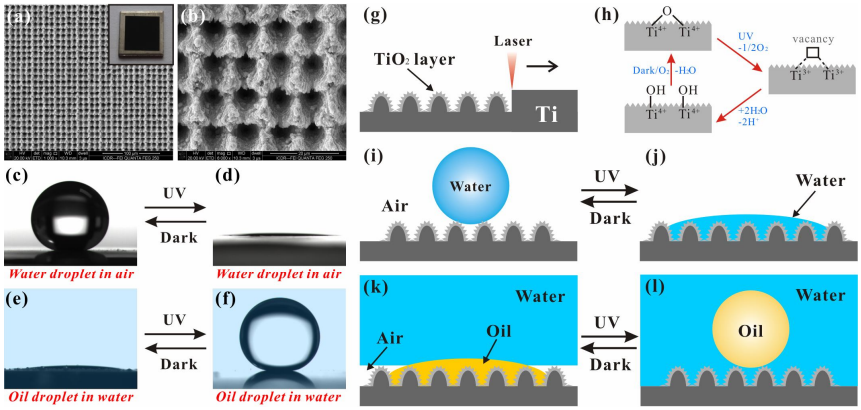

Figure 7. (a,b) SEM images of the Ti surface irradiated by femtosecond laser. (c-f) Reversible switching superhydrophobicity-superhydrophilicity and underwater superoleophilicity-superoleophobicity through alternate UV irradiation and dark storage. (g-l) Schematic illustration of the switchable wettability. (Reproduced from ref. 58 with the permission of RSC.)

With the aid of underwater superoleophobicity and ultralow oil-adhesion of femtosecond laser induced rough Si surfaces, an in-situ "mechanical hand" for oil droplet transportation was realized in water through switching the density (ρ) of the water solution.[60] As shown in Figure 8a, the setup mainly consists of one water container and two underwater superoleophobic samples (femtosecond laser irradiated Si surfaces). The whole transportation process (Figure 8b) was performed in water environment. A 15 μL oil droplet (ρ = 1.26 g/cm^3) was firstly located on the below sample (Step 1). Lowered down the above sample until it just touched the oil droplet (Step 2). Next, the sugar water (ρ = 1.52 g/cm^3) was slowly poured into the glass container to increase the ρ of water solution, switching the oil droplet from heavier to lighter than the surrounding water solution (Step 3). The oil droplet became brighter because sugar water has a closer refractive index with oil droplet than deionized water. If we lifted the above sample up, the oil droplet would be picked up since the gravity was less than the buoyancy acted on oil droplet (Step 4). Interestingly, we can also put the oil droplet back on the below sample by taking an opposite approach. Firstly, the above sample was lowered down so that the hanging oil droplet touched the below sample again (Step 5). Then, the water solution in the container was diluted by deionized water to become much lighter than the oil droplet until it returned very transparent (Step 6). The underwater oil droplet also recovered to its original brightness. Finally, with lifting the above sample up, the oil droplet detached from the above sample and stayed on the below surface (Step 7). Oil droplet can be picked up when the oil is lighter than water environment while be put down when the oil is heavier than water environment (Figure 8c). This reversible transportation can be repeated many cycles and has almost no oil loss (Figure 8d).

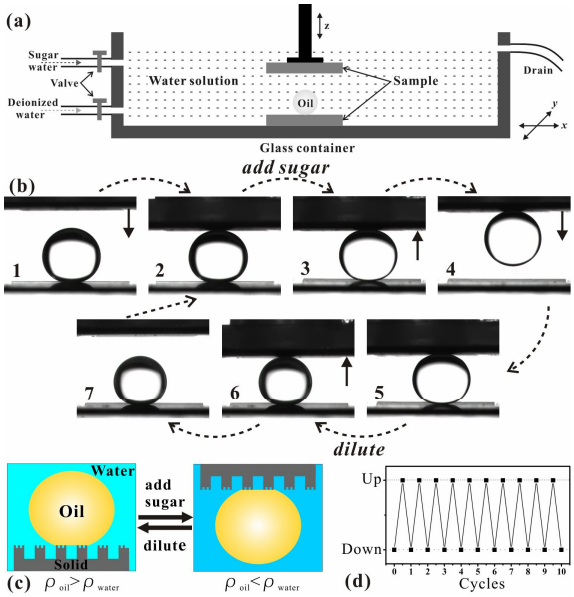

Figure 8. Underwater oil droplet transportation by underwater superoleophobic surfaces. (a) Schematic of the setup. (b) Operational process of "picking up" and "putting down" an oil droplet in water medium. (c,d) Reversibility and repeatability of the no-loss oil droplet transportation. (Reproduced from ref. 60 with the permission of Wiley.)

3. Conclusions

This paper introduces some recent developments in achieving special wettability through femtosecond laser microfabrication. Using different materials and machining methods, we can design the rough microstructure, pattern, and even chemistry on the solid substrates. Superhydrophobicity, underwater superoleophobicity, anisotropic wettability, and smart wettability have been obtained. A micro-mountain array structure is built on Si surface by femtosecond laser irradiation. After fluoroalkylsilane modification, the sample shows superhydrophobicity and ultralow water adhesion. The superhydrophobicity can also be directly obtained on hydrophobic materials, such as PDMS, without modifying by low surface energy. In addition to superhydrophobicity, the femtosecond laser induced rough Si surface also has superoleophobicity when the sample is immersed in water. A microgroove array structure is prepared by line-by-line scanning process, and the resultant surface performs anisotropic wetting and anisotropic sliding, being similar to the natural rice leaf. For some materials like Ti, oxidation process also happens with rough microstructure formation during the femtosecond laser ablation. The generated rough TiO_2 layer exhibits smart wettability; that is, superhydrophobicity-superhydrophilicity, as well as underwater superoleophilicity-superoleophobicity, can be reversible switched by alternate UV irradiation and dark storage. We believe the combination of wettability and femtosecond laser will have important potential applications in droplets/fluid manipulation, microfluidics, biomedicine, chemical and biological sensing, and so on.

Acknowledgments

This work is supported by the National Science Foundation of China under the Grant Nos. 61275008, 51335008 and 61435005, the special-funded programme on National Key Scientific Instruments and Equipment Development of China under the Grant No. 2012YQ12004706.

References

(1) K. Liu, X. Yao and L. Jiang, *Chem. Soc. Rev.*, 2010, **39**, 3240-3255.
(2) F. Xia and L. Jiang, *Adv. Mater.*, 2008, **20**, 2842-2858.
(3) T. Darmanin and F. Guittard, *J. Mater. Chem. A*, 2014, **2**, 16319-16359.
(4) X. Yao, Y. Song and L. Jiang, *Adv. Mater.*, 2011, **23**, 719-734.
(5) Z. Xue, Y. Cao, N. Liu, L. Feng and L. Jiang, *J. Mater. Chem. A*, 2014, **2**, 2445-2460.
(6) B. Bhushan, *Phil. Trans. R. Soc. A*, 2009, **367**, 1445-1486.
(7) N. J. Shirtcliffe, G. McHale and M. I. Newton, *J. Polym. Sci. Part B: Polym. Phys.*, 2011, **49**, 1203-1217.
(8) Y. Zhang, Y. Chen, L. Shi, J. Li and Z. Guo, *J. Mater. Chem.*, 2012, **22**, 799-815.
(9) P. Ragesh, V. A. Ganesh, S. V. Nair and A. S. Nair, *J. Mater. Chem. A*, 2014, **2**, 14773-14797.
(10) Y. L. Zhang, Q. D. Chen, Z. Jin, E. Kim and H. B. Sun, *Nanoscale*, 2012, **4**, 4858-4869.
(11) Y. Tian, B. Su and L. Jiang, *Adv. Mater.*, 2014, **26**, 6872-6897.
(12) B. Chang, M. Zhang, G. Qing and T. Sun, *Small*, 2015, **11**, 1097-1112.
(13) M. Liu and L. Jiang, *Adv. Funct. Mater.*, 2010, **20**, 3753-3764.
(14) X. Liu, Y. Liang, F. Zhou and W. Liu, *Soft Matter*, 2012, **8**, 2070-2086.
(15) Y. Wu, Q. Wei, M. Cai and F. Zhou, *Adv. Mater. Interf.*, 2015, **2**, 1400392.
(16) T. Sun and G. Qing, *Adv. Mater.*, 2011, **23**, H57-H77.
(17) Y. L. Zhang, H. Xia, E. Kim and H. B. Sun, *Soft Matter*, 2012, **8**, 11217-11231.
(18) S. Nishimoto and B. Bhushan, *RSC Adv.*, 2013, **3**, 671-690.
(19) X. Zhang, L. Wang and E. Levänen, *RSC Adv.*, 2013, **3**, 12003-12020.
(20) E. Stratakis, A. Rannella and C. Fotakis, *Biomicrofluidics*, 2011, **5**, 013411.
(21) Z. Chu and S. Seeger, *Chem. Soc. Rev.*, 2014, **43**, 2784-2798.
(22) L. Wen, Y. Tian and L. Jiang, *Angew. Chem. Int. Ed.*, 2015, **54**, 3387-3399.
(23) H. Teisala, M. Tuominen and J. Kuusipalo, *Adv. Mater. Interf.*, 2014, **1**, 1300026.
(24) X. M. Li, D. Reinhoudt and M. Crego-Calama, *Chem. Soc. Rev.*, 2007, **36**, 1350-1368.
(25) T. Jiang, Z. Guo and W. Liu, *J. Mater. Chem. A*, 2015, **3**, 1811-1827.
(26) A. K. Kota, J. M. Mabry and A. Tuteja, *Surface Innovations*, 2013, **1**, 71-83.
(27) Z. Xue, M. Liu and L. Jiang, *J. Polym. Sci. Part B: Polym. Phys.*, 2012, **50**, 1209-1224.
(28) X. Liu, J. Zhou, Z. Xue, J. Gao, J. Meng, S. Wang and L. Jiang, *Adv. Mater.*, 2012, **24**, 3401-3405.
(29) L. Feng, S. Li, Y. Li, H. Li, L. Zhang, J. Zhai, Y. Song, B. Liu, L. Jiang and D. Zhu, *Adv. Mater.*, 2002, **14**, 1857-1860.

(30) S. Z. Wu, D. Wu, J. Yao, Q. D. Chen, J. N. Wang, L. G. Niu, H. H. Fang and H. B. Sun, *Langmuir*, 2010, **26**, 12012-12016.
(31) D. Wu, J. N. Wang, S. Z. Wu, Q. D. Chen, S. Zhao, H. Zhang, H. B. Sun and L. Jiang, *Adv. Funct. Mater.*, 2011, **21**, 2927-2932.
(32) D. Wang, Y. Liu, X. Liu, F. Zhou, W. Liu and Q. Xue, *Chem. Commun.*, 2009, 7018-7020.
(33) D. Wang, X. Wang, X. Liu and F. Zhou, *J. Phys. Chem. C*, 2010, **114**, 9938-9944.
(34) L. Zhang, Z. Zhang and P. Wang, *NPG Asia Mater.*, 2012, **4**, e8.
(35) Z. Cheng, H. Lai, Y. Du, K. Fu, R. Hou, C. Li, N. Zhang and K. Sun, *ACS Appl. Mater. Interfaces*, 2014, **6**, 636-641.
(36) T. Sun, G. Wang, L. Feng, B. Liu, Y. Ma, L. Jiang and D. Zhu, *Angew. Chem. Int. Ed.*, 2004, **43**, 357-360.
(37) F. Xia, L. Feng, S. Wang, T. Sun, W. Song, W. Jiang and L. Jiang, *Adv. Mater.*, 2006, **18**, 432-436.
(38) S. Lee, W. Kim and K. Yong, *Adv. Mater.*, 2011, **23**, 4398-4402.
(39) X. Hong, X. Gao and L. Jiang, *J. Am. Chem. Soc.*, 207, **129**, 1478-1479.
(40) D. Wu, S. Z. Wu, Q. D. Chen, Y. L. Zhang, J. Yao, X. Yao, L. G. Niu, J. N. Wang, L. Jiang and H. B. Sun, *Adv. Mater.*, 2011, **23**, 545-549.
(41) S. Zhao, H. Xia, D. Wu, C. Lv, Q. D. Chen, K. Ariga, L. Q. Liu and H. B. Sun, *Soft Matter*, 2013, **9**, 4236-4240.
(42) P. Guo, Y. Zheng, C. Liu, J. Ju and L. Jiang, *Soft Matter*, 2012, **8**, 1770-1775.
(43) Y. Cai, L. Lin, Z. Xue, M. Liu, S. Wang and L. Jiang, *Adv. Funct. Mater.*, 2014, **24**, 809-816.
(44) Y. Li, E. J. Lee and S. O. Cho, *J. Phys. Chem. C*, 2007, **111**, 14813-14817.
(45) Y. Li, X. J. Huang, S. H. Heo, C. C. Li, Y. K. Choi, W. P. Cai and S. O. Cho, *Langmuir*, 2007, **23**, 2169-2174.
(46) J. Li, X. Liu, Y. Ye, H. Zhou and J. Chen, *J. Phys. Chem. C*, 2011, **115**, 4726-4729.
(47) Z. Cheng, H. Lai, Y. Du, K. Fu, R. Hou, N. Zhang and K. Sun, *ACS Appl. Mater. Interfaces.*, 2013, **5**, 11363-11370.
(48) D. Wu, S. Z. Wu, Q. D. Chen, S. Zhao, H. Zhang, J. Jiao, J. A. Piersol, J. N. Wang, H. B. Sun and L. Jiang, *Lab Chip*, 2011, **11**, 3873-3879.
(49) M. Im, H. Im, J. H. Lee, J. B. Yoon and Y. K. Choi, *Soft Matter*, 2010, **6**, 1401-1404.
(50) E. Bormashenko, R. Grynyov, Y. Bormashenko and E. Drori, *Sci. Rep.*, 2012, **2**, 741.
(51) J. Zhang and S. Seeger, *Angew. Chem. Int. Ed.*, 2011, **50**, 6652-6656.
(52) M. Guo, B. Ding, X. Li, X. Wang, J. Yu and M. Wang, *J. Phys. Chem. C*, 2010, **114**, 916-921.
(53) H. S. Lim, J. H. Baek, K. Park, H. S. Shin, J. Kim and J. H. Cho, *Adv. Mater.*, 2010, **22**, 2138-2141.
(54) F. Chen, D. Zhang, Q. Yang, J. L. Yong, G. Du, J. Si, F. Yun and X. Hou, *ACS Appl. Mater. Interfaces*, 2013, **5**, 6777-6792.
(55) J. L. Yong, Q. Yang, F. Chen, D. Zhang, U. Farooq, G. Du and X. Hou, *J. Mater. Chem. A*, 2014, **2**, 5499-5507.
(56) J. L. Yong, F. Chen, Q. Yang, D. Zhang, U. Farooq, G. Du and X. Hou, *J. Mater. Chem. A*, 2014, **2**, 8790-8795.
(57) J. L. Yong, F. Chen, Q. Yang, G. Du, C. Shan, H. Bian, U. Farooq and X. Hou, *J. Mater. Chem. A*, 2015, **3**, 9379-9384.
(58) J. L. Yong, F. Chen, Q. Yang, U. Farooq and X. Hou, *J. Mater. Chem. A*, 2015, **3**,

10703-10709.
(59) J. L. Yong, F. Chen, Q. Yang, Y. Fang, J. Huo and X. Hou, *Chem. Commun.*, 2015, **51**, 9813-9816.
(60) J. L. Yong, Q. Yang, F. Chen, H. Bian, G. Du, U. Farooq and X. Hou, *Adv. Mater. Interf.*, 2015, **2**, 1400388.
(61) D. Zhang, F. Chen, Q. Yang, J. L. Yong, H. Bian, Y. Ou, J. Si, X. Meng and X. Hou, *ACS Appl. Mater. Interfaces*, 2012, **4**, 4905-4912.
(62) J. L. Yong, F. Chen, Q. Yang, D. Zhang, G. Du, J. Si, F. Yun and X. Hou, *J. Phys. Chem. C*, 2013, **117**, 24907-24912.
(63) J. L. Yong, F. Chen, Q. Yang, D. Zhang, H. Bian, G. Du, J. Si, X. Meng and X. Hou, *Langmuir*, 2013, **29**, 3274-3279.
(64) J. L. Yong, F. Chen, Q. Yang, G. Du, H. Bian, D. Zhang, J. Si, F. Yun and X. Hou, *ACS Appl. Mater. Interfaces*, 2013, **5**, 9382-9385.
(65) P. Roach, N. J. Shirtcliffe and M. I. Newton, *Soft Matter*, 2008, **4**, 224-240.
(66) K. Liu and L. Jiang, *Nano Today*, 2011, **6**, 155-175.
(67) C. H. Xue and J. Z. Ma, *J. Mater. Chem. A*, 2013, **1**, 4146-4161.
(68) M. Nosonovsky and B. Bhushan, *J. Phys.: Condens. Matter*, 2008, **20**, 225009.
(69) W. Barthlott and C. Neinhuis, *Planta*, 1997, **202**, 1-8.
(70) T. Baldacchini, J. E. Carey, M. Zhou and E. Mazur, *Langmuir*, 2006, **22**, 4917-4919.
(71) V. Zorba, E. Stratakis, M. Barberoglou, E. Spanakis, P. Tzanetakis, S. Anastasiadis and C. Fotakis, *Adv. Mater.*, 2008, **20**, 4049-4054.
(72) J. L. Yong, Q. Yang, F. Chen, D. Zhang, H. Bian, Y. Ou, G. Du and X. Hou, *Appl. Phys. A*, 2013, **111**, 243-249.
(73) F. Chen, D. Zhang, Q. Yang, X. Wang, B. Dai, X. Li, X. Hao, Y. Ding, J. Si and X. Hou, *Langmuir*, 2011, **27**, 359-365.
(74) A. B. D. Cassie and S. Baxter, *Trans. Faraday. Soc.*, 1944, **40**, 546-551.
(75) S. Wang and L. Jiang, *Adv. Mater.*, 2007, **19**, 3423-3424.
(76) J. L. Yong, Q. Yang, F. Chen, D. Zhang, G. Du, H. Bian, J. Si, F. Yun and X. Hou, *Appl. Surf. Sci.*, 2014, **288**, 579-583.
(77) M. Liu, S. Wang, Z. Wei, Y. Song and L. Jiang, *Adv. Mater.*, 2009, **21**, 665-669.
(78) X. Deng, L. Mammen, H. J. Butt and D. Vollmer, *Science*, 2012, **335**, 67-70.
(79) P. A. Levkin, F. Svec and J. M. J. Fréchet, *Adv. Funct. Mater.*, 2009, **19**, 1993-1998.
(80) J. L. Yong, F. Chen, Q. Yang, U. Farooq, H. Bian, G. Du and X. Hou, *Appl. Phys. A*, 2015, **119**, 837-844.
(81) M. Gleiche, L. F. Chi and H. Fuchs, *Nature*, 2000, **403**, 173-175.
(82) S. G. Park, J. H. Moon, H. C. Jeon and S. M. Yang, *Soft Matter*, 2012, **8**, 4567-4570.
(83) E. Mele, S. Girardo and D. Pisignano, *Langmuir*, 2012, **28**, 5312-5317.
(84) J. Y. Chung, J. P. Youngblood and C. M. Stafford, *Soft Matter*, 2007, **3**, 1163-1169.
(85) A. Y. Vorobyev and C. L. Guo, *Appl. Phys. Lett.*, 2009, **94**, 224102.
(86) Y. M. Zheng, H. Bai, Z. B. Huang, X. L. Tian, F. Q. Niu, Y. Zhao, J. Zhai and L. Jiang, *Nature*, 2010, **463**, 640-643.
(87) J. C. Baret and M. M. J. Decré, *Langmuir*, 2007, **23**, 5200-5204.
(88) J. Ju, H. Bai, Y. M. Zheng, T. Y. Zhao, R. C. Fang and L. Jiang, *Nat. Commun.*, 2012, **3**, 1247.
(89) A. Y. Vorobyev and C. L. Guo, *J. Appl. Phys.*, 2010, **108**, 123512

(90) K. Khare, S. Herminghaus, J. C. Baret, B. M. Law, M. Brinkmann and R. Seemann, *Langmuir*, 2007, **23**, 12997-13006.
(91) Z. Yoshimitsu, A. Nakajima, T. Watanabe and K. Hashimoto, *Langmuir*, 2002, **18**, 5818-5822.
(92) J. L. Yong, F. Chen, Q. Yang, U. Farooq, H. Bian, G. Du and X. Hou, *Appl. Phys. Lett.*, 2014, **105**, 071608.
(93) Y. Zheng, X. Gao and L. Jiang, *Soft Matter*, 2007, **3**, 178-182.
(94) J. L. Yong, Q. Yang, F. Chen, D. Zhang, G. Du, H. Bian, J. Si and X. Hou, *RSC Adv.*, 2014, **4**, 8138-8143.
(95) I. A. Larmour, S. E. J. Bell and G. C. Saunders, *Angew. Chem.*, 2007, **119**, 1740-1742.
(96) K. Liu, M. Cao, A. Fujishima and L. Jiang, *Chem. Rev.* **2014**, *114*, 1044-1094.
(97) R. Wang, K. Hashimoto, A. Fujishima, M. Chikuni, E. Kojima, A. Kitamura, M. Shimohigoshi and T. Watanabe, *Nature* **1997**, *388*, 431-433.
(98) Y. Li, G. Duan, G. Liu and W. Cai, *Chem. Soc. Rev.* **2013**, *42*, 3614-3627.
(99) Y. Li, T. Sasaki, Y. Shimizu and N. Koshizaki, *J. Am. Chem. Soc.* **2008**, *130*, 14755-14762.
(100) Y. Li, N. Koshizaki, H. Wang and Y. Shimizu, *ACS NANO* **2011**, *5*, 9403-9412.
(101) Y. Li, T. Sasaki, Y. Shimizu and N. Koshizaki, *Small* **2008**, 2286-2291.

A table of contents entry

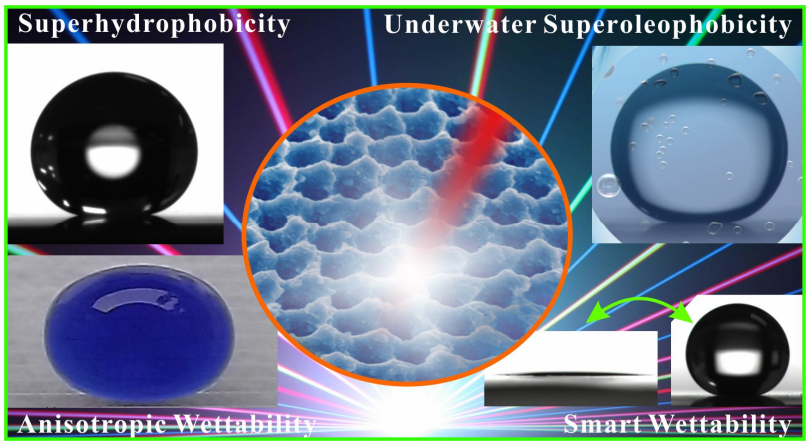

This paper introduces four typical aspects of femtosecond laser induced special wettability: superhydrophobicity, underwater superoleophobicity, anisotropic wettability, and smart wettability.

A photograph and biography of myself and my co-authors

Dr Jiale Yong is currently a PhD candidate in Prof. Feng Chen's research group at Xi'an Jiaotong University. He received his BS degree from Xi'an Jiaotong University in 2011. His research interests include femtosecond laser microfabrication, controlling wettability of solid surfaces, and bioinspired designing superhydrophobic and superoleophobic interfaces.

Prof. Feng Chen is a full professor of Electronic Engineering at Xi'an Jiaotong University, where he directs the Femtosecond Laser Laboratory. He received the BS degree in physics from Sichuan University, China, in 1991, and then began to work for Chinese Academy of Science (1991 to 2002), where he was promoted to a full professor in 1999. He received the PhD in Optics from Chinese Academy of Science in 1997. In 2002, he joined Xi'an Jiaotong University, where he became a group leader. His current research interests are femtosecond laser microfabrication and bionic microfabrication.

Prof. Qing Yang received her BS degree in Photoelectron Science and Technology in 1992 from Sichuan University. In 2009, she received her PhD from Xi'an Institute of Optics and Fine Mechanics, Chinese Academy of Science. She is currently an associate professor at Xi'an Jiaotong University. Her current research interests are femtosecond laser fine process, microfluidic biochips, and micro-photonics.

Prof. Xun Hou received his BS degree in Physics from Northwest University, China, in 1959. From Oct. 1979 to Nov. 1981, he worked at Imperial College in England as a visiting scholar. He was elected as an academician of Chinese Academy of Sciences in 1991. He presently is a professor of Xi'an Jiaotong University, and he is also the director of the Shaanxi Key Laboratory of Photonics Technology for Information. His research interests mainly focus on photoelectronic materials and devices.